Lawn Structured Triboelectric Nanogenerators for Scavenging Sweeping Wind Energy on Rooftops

Lei Zhang, Binbin Zhang, Jun Chen, Long Jin, Weili Deng, Junfeng Tang, Haitao Zhang, Hong Pan, Minhao Zhu, Weiqing Yang, and Zhong Lin Wang**

With the increasing greenhouse effect due to increased carbon emissions and limited fossil fuels available for the next century, searching for new energy sources is a major challenge and necessary for the sustainable development of human civilization. Over decades, an increasing research effort has been committed to developing renewable and green energy technologies.[1] Wind, available in huge quantities, is one of the cleanest and most sustainable energy sources that nature provides. Conventional mechanisms for harvesting wind energy are mainly limited to transduction based on electromagnetic effect by usage of wind turbines.[2,3] Widespread usage of this technique is likely to be shadowed by possible limitations, such as structure complexity, fabrication of high-quality materials, large weight/density, and volume as well as high cost of installation.

Recently, rooting in a coupling effect of contact electrification and electrostatic induction, the triboelectric nanogenerator (TENG) has been proved to be an effective and robust approach for ambient mechanical energy harvesting.[4–14] Mainly utilizing conventional polymer thin film materials, the TENGs have been featured as extremely low-cost, easy to fabricate and easy to be scaled up, and its performance is superior to other approaches of its kind.[15–26] TENG based wind energy harvesters were developed recently by using the wind induced membrane vibration, however, the prototypes can only work under a certain wind direction.[27–31] However, most ambient wind does not have a constant direction, which may even drift over time, making the previous reports unsuitable in most circumstances.

Here, we present a flexible and transparent TENG to harvest energy from natural wind at arbitrary wind blowing direction. Reliance on the vertically free-standing polymer strips, which consist of indium tin oxide (ITO) coated polyethylene terephthalate (PET) thin film, the laminar TENGs array holds a kelp forest morphology and each single strip could sway independently to cause a contact-separation when the natural wind passes by. For a systematical study, a high speed camera was employed to clearly capture the working states and interaction between two adjacent TENGs. The vertically free-standing polymer strips hold a vibration frequency as high as 154 Hz under wind blowing. This high-frequency swing assures sufficient contact-separation among strips as required for high electric output. With a strip size of 10 × 2 cm and under an airflow velocity of 27 ms^{-1}, two adjacent strips with rooftop area of 2 × 0.7 cm can deliver an open-circuit voltage, short-circuit current, and power density up to 98 V, 16.3 μA, and 2.76 Wm^{-2} ($P_d = P/S_{rooftop}$, see the Supporting Information for detailed calculation), respectively. The power generated can instantaneously light up an advertisement board. In addition, an array of TENGs consisting of 60 strips was developed to harvest energy from natural wind. After installation of the device onto a rooftop, the generated rooftop power density is up to 2.37 Wm^{-2} and its electricity is capable of simultaneously lighting up 60 light-emitting diode (LED) bulbs connect in series as a self-powered advertisement board. If a common house with the rooftop area size of about 300 m^2 are installed with ten-layered lawn structured TENGs, the whole wind energy harvester is expected to deliver an electrical energy of 7.11 KW, which corresponds to a power density of 23.7 Wm^{-2}. It unambiguously demonstrated the capability of TENG acting as a sustainable power source for home-used electronics. This work not only presents a novel approach in the field of wind energy harvesting, but also a solid step towards self-powered home technology.

The TENGs array has a kelp-forest-like morphology, as schematically illustrated in **Figure 1**a. Figure 1b shows a basic unit of the TENG, which is a pair of strips, consisted of ITO coated PET with an end anchored onto the substrate and the other end stayed free-standing. Tens of strips orderly arrayed to form a wind farm for environmental wind energy harvesting. PET was selected as the backbone of the strip, mainly owning to its decent strength, low cost, good machinability as well as the decent electron affinity. In addition, to enhance the effective contact area for an improved output performance, PET polymer nanowires were created on the exposed PET surface by a top-down method of reactive ion etching.[23,25] An SEM image of PET nanowires was displayed in the Figure 1c. As illustrated in Figure 1d, the TENG can be easily equipped to the rooftops or the fence along the railroad tracks. A detailed fabrication process of the TENG is presented in the Experimental Section.

Dr. L. Zhang, B. Zhang, L. Jin, Dr. W. Deng, J. Tang, Dr. H. T. Zhang, H. Pan, Prof. M. Zhu, Prof. W. Yang
Key Laboratory of Advanced Technologies of Materials (Ministry of Education)
School of Materials Science and Engineering
Southwest Jiaotong University
Chengdu 610031, China
E-mail: wqyang@swjtu.edu.cn
Dr. J. Chen, Prof. Z. L. Wang
School of Materials Science and Engineering
Georgia Institute of Technology
Atlanta, GA 30332, USA
E-mail: zlwang@gatech.edu
Prof. Z. L. Wang
Beijing Institute of Nanoenergy and Nanosystems
Chinese Academy of Sciences
Beijing 100085, China

DOI: 10.1002/adma.201504462

© 2015 WILEY-VCH Verlag GmbH & Co. KGaA, Weinheim

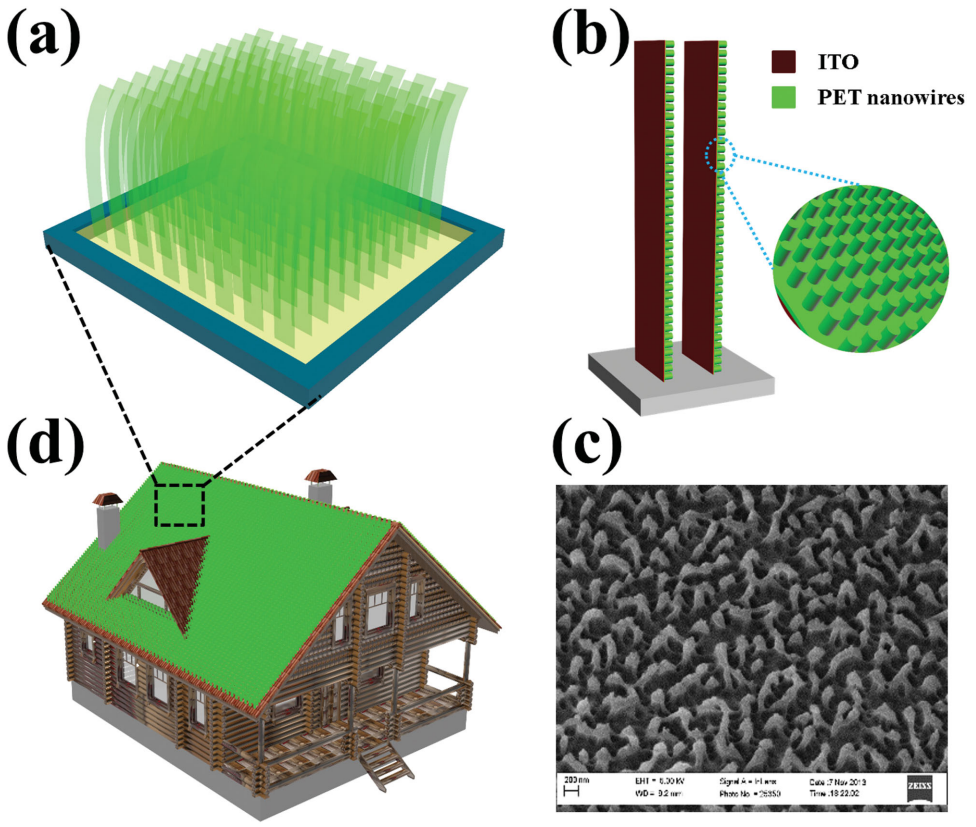

Figure 1. Lawn structured triboelectric nanogenerator. a) Schematical illustration of the TENG, which has a kelp-forest-like morphology. b) A basic unit of the TENG, which is a pair of strips, which is consisted of ITO coated PET with an end anchored onto the substrate and the other end stayed free-standing. c) SEM image of PET nanowires. d) A sketch shows that the TENG can be easily equipped to the rooftops for natural wind energy harvesting.

The basic working principle of the TENG is based on the coupling between contact electrification and electrostatic induction.[32–40] In virtue of the opposite triboelectric polarities between ITO and PET, the electron is injected from ITO into PET once the two are brought into contact with each other. Then an electrical potential difference will be established in subsequent separation process that will drive the free electrons to flow back and forth across the electrodes, and thus a current in an alternating manner will emerge in the external circuit. When the natural wind blows across the TENG array, the initiated swing of the free-standing strips will cause physical contact-separations among them. Hence, the wind energy is converted into electricity. In order to consolidate the working principle of the TENG, COMSOL was employed to simulate the periodic potential variation between the two electrodes upon contact and separation, as demonstrated in **Figure 2**a1–e1. The continuous variation of the potential distribution is visualized in Movie 1 of the Supporting Information.

To clearly picture the working states of the TENG, a high-speed camera with a frame rate of 2000 Hz was employed to capture the dynamic process of the contact-separation process between two adjacent flexible strips. At the origin state, the strips are bent to contact together under a steady and successive wind blowing, as shown in Figure 2a2,b2. Subsequently, the bent strips will go through the propagation state (Figure 2c2) to separation state (Figure 2d2) owing to the elastic restoration as well as the atmospheric pressure between two adjacent strips. As the separation distances between the two strips increases, the atmospheric pressure will bring them down once again. Therefore, the strips convert from propagation state (Figure 2e2) to contact state (Figure 2f2) again. Moreover, the strips present a damping property as result of its decent elasticity modulus with the air-flow off. The dynamic process for the air-flow driven swing behaviour of the strips is visualized in Movie 2 of the Supporting Information. In addition, the TENG can also work under an on and off wind circumstance, as shown in Figures S1 and S2 of the Supporting Information.

The electric output of the as-fabricated TENG is highly related to the wind induced strips contact-separation process, thus the designed gap distance between two strips is a critical parameter that will shows great impact on the device output performance. As indicated in **Figure 3**a,b, experimentally under a fixed wind flow velocity, the peak output is an increasing function of the gap distance till an optimal distance emerges (7 mm). And then, the electric output decreases as the gap distance increases. In the meanwhile, a further step was taken to investigate the dependence of the electrical output of the TENG on the wind blowing angle. A wind blowing angle is the angle between the wind direction and the stripes surface normal direction, which is illustrated in Figure S3a of the Supporting Information. As shown in Figure S3b of the Supporting Information, although the electrical output of TENG

© 2015 WILEY-VCH Verlag GmbH & Co. KGaA, Weinheim
Adv. Mater. **2015**,
DOI: 10.1002/adma.201504462

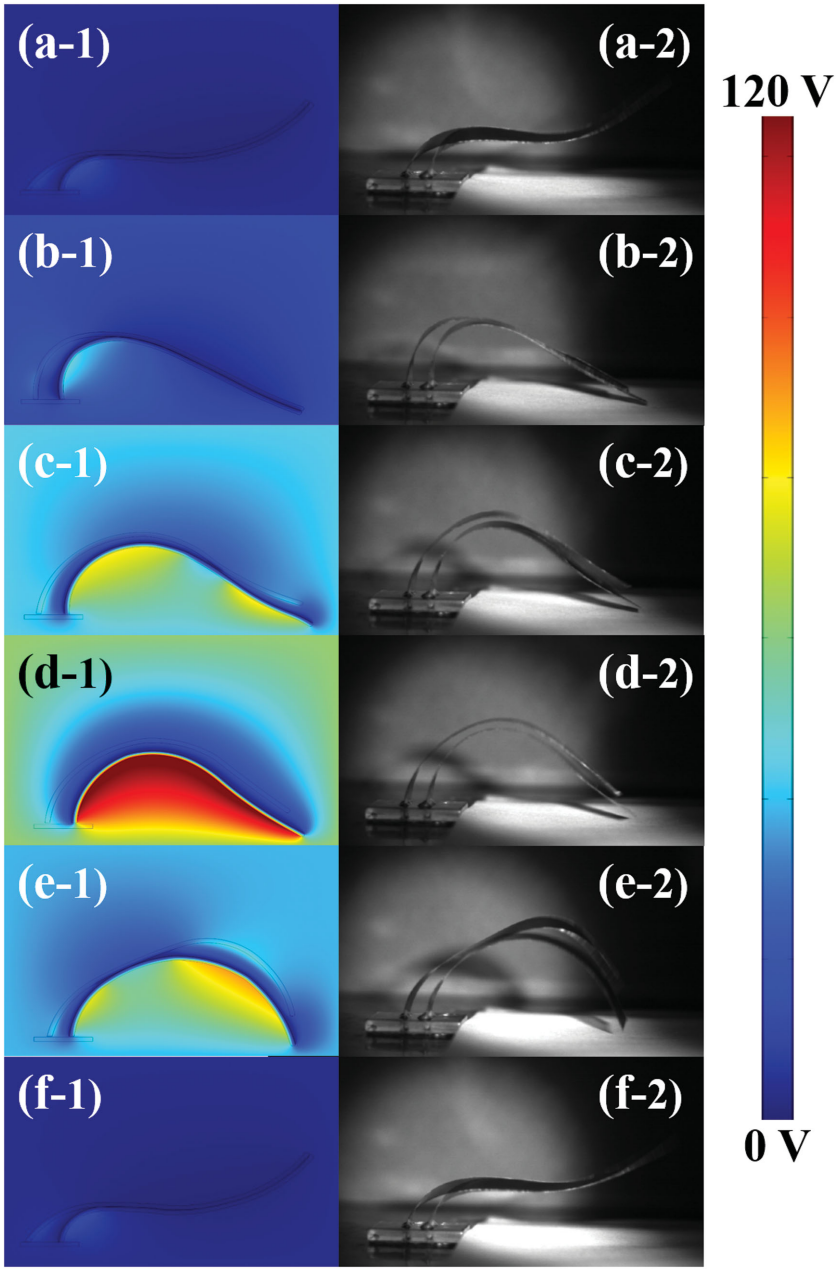

Figure 2. Sketch that illustrates the fluttering behavior and operating principle of the TENG. a–f) Left: 2D simulation of the potential distribution of two adjacent stripes by COMOSOL. Right: Fluttering behavior of two adjacent strips with dimensions 10 × 2 cm was captured by a high-speed camera under a flow velocity of 27 ms^{-1}.

decreased with the increasing of the blowing angles and it is maximized at the blowing angle of 0°, it clearly demonstrated that the lawn structured TENG can harvest the wind energy from arbitrary wind direction. Furthermore, the wind flow velocity is also another parameter that will largely influence the electrical output of the TENG. Figure 3c,d, shows the dependence of the open-circuit voltage and short-circuit current, respectively, on the wind flow velocities in a wide range of from 0 to 27 ms^{-1} with a fixed stripe gap distance of 7 mm. (Relevant wind scale and wind speed has been presented in Table S1, Supporting Information.) It is obviously revealing that the higher wind velocity will result in a higher electric output. Moreover, the vertically free-standing polymer strips hold an increasing vibration frequency with the wind blowing velocities (please see Figure S4, Supporting Information), which presents a vibration frequency as high as 154 Hz under the wind blowing. Such high-frequency swing assures sufficient contact-separation among strips, and thus a decent electric output. Apart from this, electrical output of TENG can be altered by controlling not only a wind force but also a contact area. Thus, we made an in-depth investigation by varying the length and width of a stripes of the lawn structured TENG at a fixed wind velocity of 17 m s^{-1} (Figures S5 and S6, Supporting Information), showing this lawn TENG can raise its power output by the change of device dimension. Resistors were also utilized as external loads to further investigate the output power of the TENG at a wind velocity of 27 m s^{-1}. As displayed in Figure 3e, the current amplitude drops with increasing the load resistances owing to the Ohmic loss, while the voltage follows a reverse trend. As a result, the instantaneous peak power is maximized at a load resistance of 10 MΩ, corresponding to a peak power density ($P_d = UI/S_{rooftop}$) of 2.76 Wm^{-2} (Figure 3f).

A key challenge to TENG is its relatively low output current.[41–43] In order to enhance the total current output of the TENG, all of the unit cells are electrically connected in parallel. To study the output performance of the TENG and dig out the output law, the dependence of the unit number on the electric output was systematically investigated. Under a constant wind velocity of 27 ms^{-1}, the electric output of the TENG was respectively measured with N = 1, 2, 4 (**Figure 4**a–c). These corresponding sketches are presented in Figure 4a1,b1,c1. As shown, the TENG produces an open-circuit voltage of 96 V at N = 1 (Figure 4a2), 79 V at N = 2 (Figure 4b2), and 70 V at N = 4 (Figure 4c2). A slightly decreasing of the voltage output is mainly attributed to the difficulty of the synchronization of the unit cells.[43] In the meanwhile, the peak values of short-circuit current (I_{sc}) reaches up to 16.3 μA at N = 1 (Figure 4a3), 42.3 μA at N = 2 (Figure 4b3) and 71.3 μA at N = 4 (Figure 4c3), which shows an obvious increasing of the output current as the increase of the unit number. In addition, the output current has an alternating behavior with asymmetrical amplitudes, with the larger peaks corresponding to the process in which the contact surfaces move towards each other, while the smaller ones are generated as the contact surfaces move apart. Last but not least,

© 2015 WILEY-VCH Verlag GmbH & Co. KGaA, Weinheim

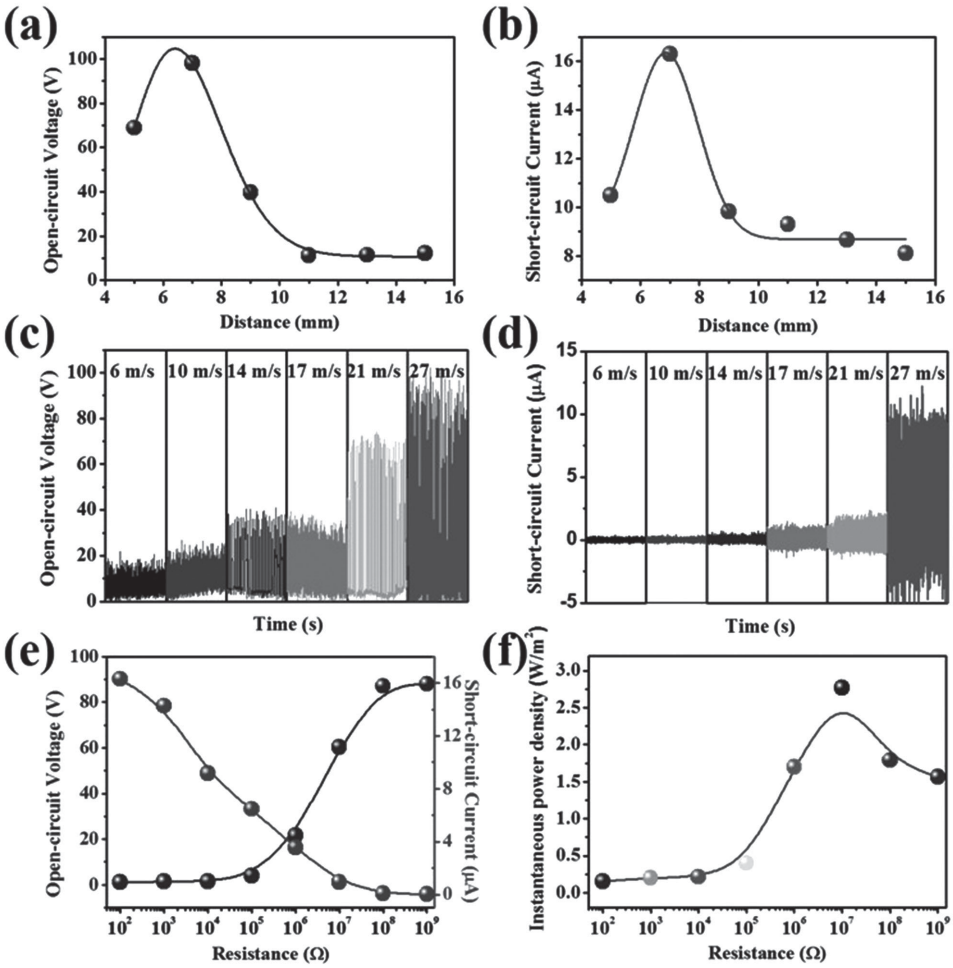

Figure 3. Influence of flow velocity and stripe gap distance on the electrical output. a,b) Electrical output performance of the TENG with different films' gap distance from 3 to 15 mm. a) Open-circuit voltage, b) short-circuit current. c,d) Electrical output performances of the TENG with different flow velocity from 6 mm to 27 mm. (c) Open-circuit voltage, (d) short-circuit current. (e) Dependence of the voltage and current output on the external load resistance. The points represent peak value of electric signals while the lines are the fitted results; f) Dependence of the peak power output on the resistance of the external load, indicating maximum power output when $R = 10$ M Ω. The curve is a fitted result.

we investigated the performance of TENG under the circumstances of wet and moisture. As shown in **Figure 5**a,b, both V_{OC} and I_{SC} of TENG gradually decreased with the increase of humidity at the various wind velocities. When the humidity recover the normal values, the electrical output of TENG is easy to regain. Moreover, the static contact angles of ITO and PET surface were measured to be 95.1° and 104.6° (Figure 5c,d), respectively, which shows a slightly hydrophobicity of the TENG.[44] With this surface wettability, under a wind blow and the induced vibration of the strips, the water or rain drops on the TENG surface are easily removed. This deduced self-reinstating process is presented in Figure S7 of the Supporting Information.

To prove the capacity of TENG for ambient wind energy harvesting as a sustainable power source, three sets of practical applications were demonstrated (see the videos in Supporting Information). As shown in **Figure 6**a,b, the TENG with $N = 1$ was driven by the blower to harvest wind energy at the wind velocity of 27 ms^{-1}, seven light-emitting diode (LED) bulbs were simultaneously and continuously illuminated (Movie 3, Supporting Information). Furthermore, as shown in Figure 6c,d, a TENG with $N = 60$ and a roof top dimension of 12 × 15 cm was developed. Under the blowing by an electric fan, this TENG produced the power density of 2.37 Wm^{-2} and 60 light-emitting diode (LED) bulbs were lighted up simultaneously (Movie 4, Supporting Information). In addition, based on this, a model house was developed as presented in Figure 6e,f. A display board was illuminated by this house (Movie 5, Supporting Information), which unambiguously demonstrated the capability of our TENG acting as a sustainable power source for home-use electronics. Supposing a common house with the rooftop area of about 300 m^2 that are installed with prolonged ten-layer lawn structured TENGs (Figure S8, Supporting Information), an electrical energy of 7.11 KW with a power density of 23.7 Wm^{-2} is expected. The demonstrations evidently show the tremendously potential of the TENG with wide applications by harvesting the natural wind energy, especially in remote mountain areas.

© 2015 WILEY-VCH Verlag GmbH & Co. KGaA, Weinheim
Adv. Mater. **2015**,
DOI: 10.1002/adma.201504462

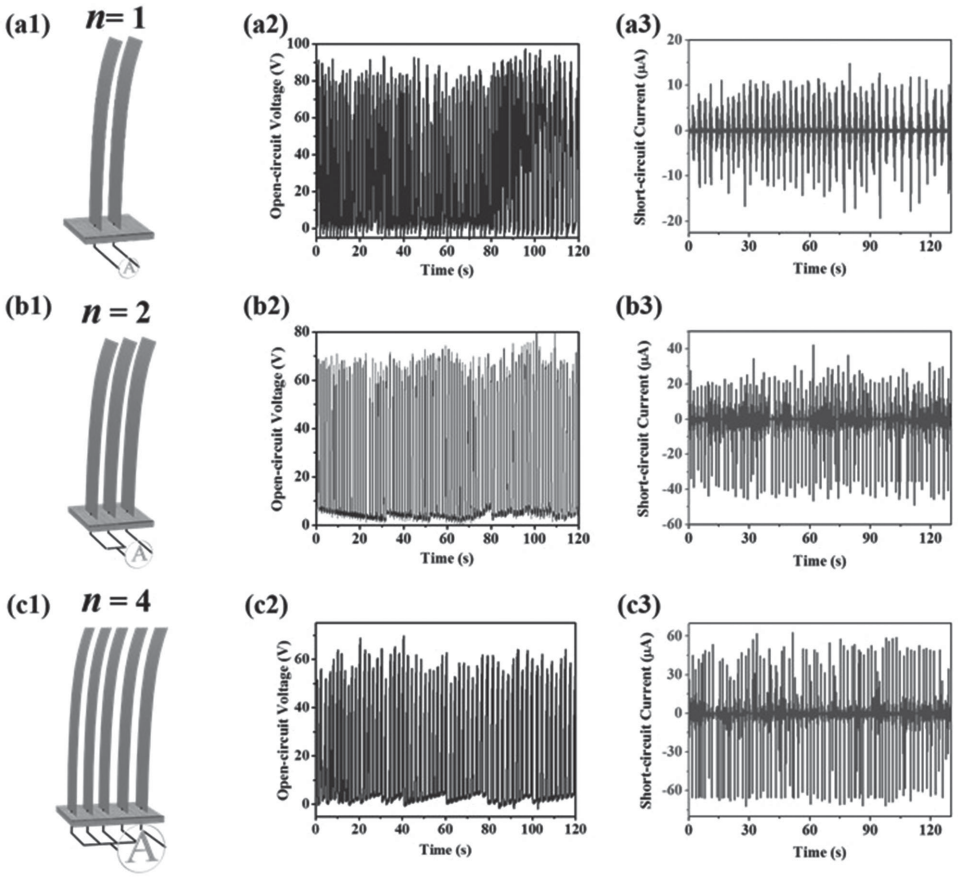

Figure 4. Electrical measurement of the Integrated TENG with $N = 1$, 2, and 4, respectively. a1–c1) Illustration to show the electrical connection mode of the unit cells. a2–c2) Open-circuit voltage (V_{OC}). a3–c3) Short-circuit current (I_{SC}).

In summary, we present a simple, low-cost, transparent and completely flexible TENG for environmental wind energy harvesting. With surface nanostructure modification, the rationally designed TENG with $N = 1$ produces an open-circuit voltage up to 98 V and a short-circuit current of 16.3 μA, corresponding to a current density of 0.12 Am^{-2} and power density of 2.76 Wm^{-2}. The output power is shown to greatly increase with the unit number. Furthermore, a high speed camera was employed to monitor the working process. With a unit number of 60, the TENG was demonstrated to output the rooftop power density of 2.37 Wm^{-2} and illuminate 60 LEDs. The device was also installed onto a model house: the harvested power from natural wind can instantaneously light up an advertisement display board. Featured as independent of the wind direction, this work not only presents a novel approach in the field of wind energy harvesting, but also a solid step towards self-powered home technology.

Experimental Section

Preparation of ITO-PET Nanowires Film: The process to prepare the ITO–PET nanowire was divided into two steps: (1) Nanowire-based PET surface modification. (2) The depositing of ITO electrode. A 300 nm thick ITO was deposited on the other side of the as-prepared PET nanowire film played dual roles as a contact electrode and a back electrode.

Nanowire-Based PET Surface Modification: First, a 125 mm thick terephthalate (PET) film was prepared with the desired dimensions and a layer of 100 nm copper was deposit on it for the etching process. Then the ICP etching was applied to fabricate the aligned PET nanowire which will largely enhance the contact electrification on one side of the film. Ar, O_2, and CF_4 were injected into the ICP chamber with a special flow ratio of 15.0, 10.0, and 30.0 sccm under 400 W RF power and 100 W bias power. Subsequently, 100 nm thick copper was etched for 40s to get the PET nanowires.

Fabrication of the TENG: First, the strips were cut out with dimensions of 10 × 2 cm. Then lead wires were connected to the surface of ITO. The acrylic pedestal was shaped by using a laser cutting machine. Finally, the strips were inserted into the pedestal.

Characterization of the TENG: The morphologies of the samples were characterized by field emission scanning electron microscopy (JEDL-JSM-7001F). The dynamic process of the contact-separation was captured by a high-speed camera with a frame rate of 2000 Hz (Photron UX50). The static contact angles of ITO-PET nanowire film were measured by a contact angle measuring instrument (Krüss FM3200). The output current signals of TENG were measured by a low-noise current preamplifier (Stanford Research SR570). The output voltage signals of the triboelectric nanogenerator were measured by a low-noise voltage preamplifier (Keithley 6514 system electrometer).

Supporting Information

Supporting Information is available from the Wiley Online Library or from the author.

© 2015 WILEY-VCH Verlag GmbH & Co. KGaA, Weinheim

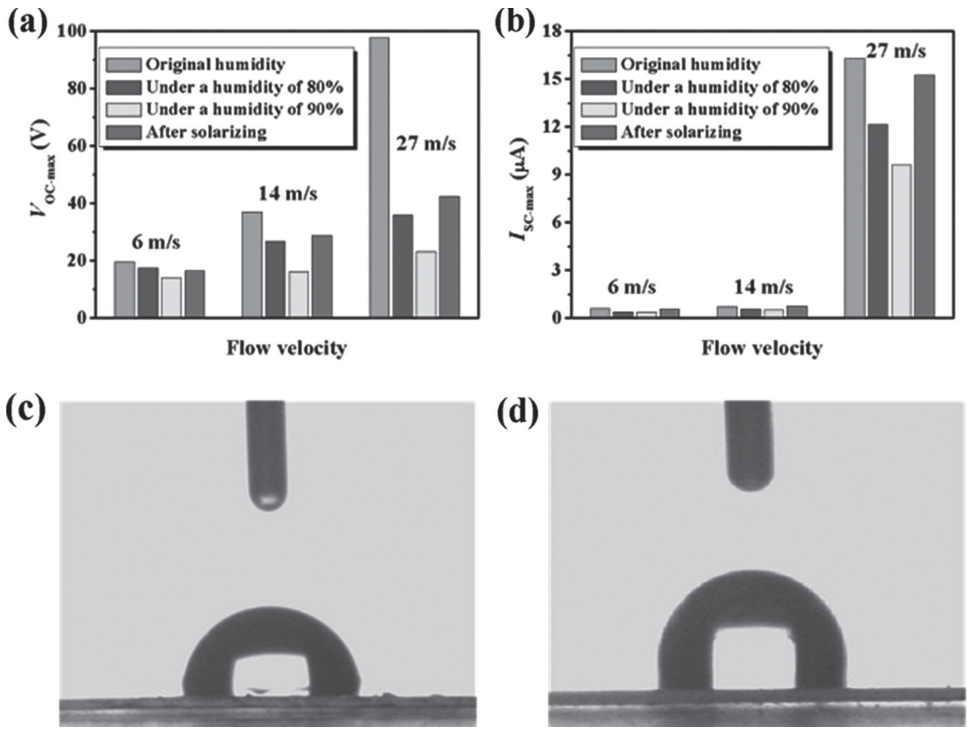

Figure 5. Influence of the humidity on the electrical output of the TENG. a) Open-circuit voltage, b) short-circuit current of the TENG under different humidity. Static contact angle measurement for the c) ITO film and b) PET film surface.

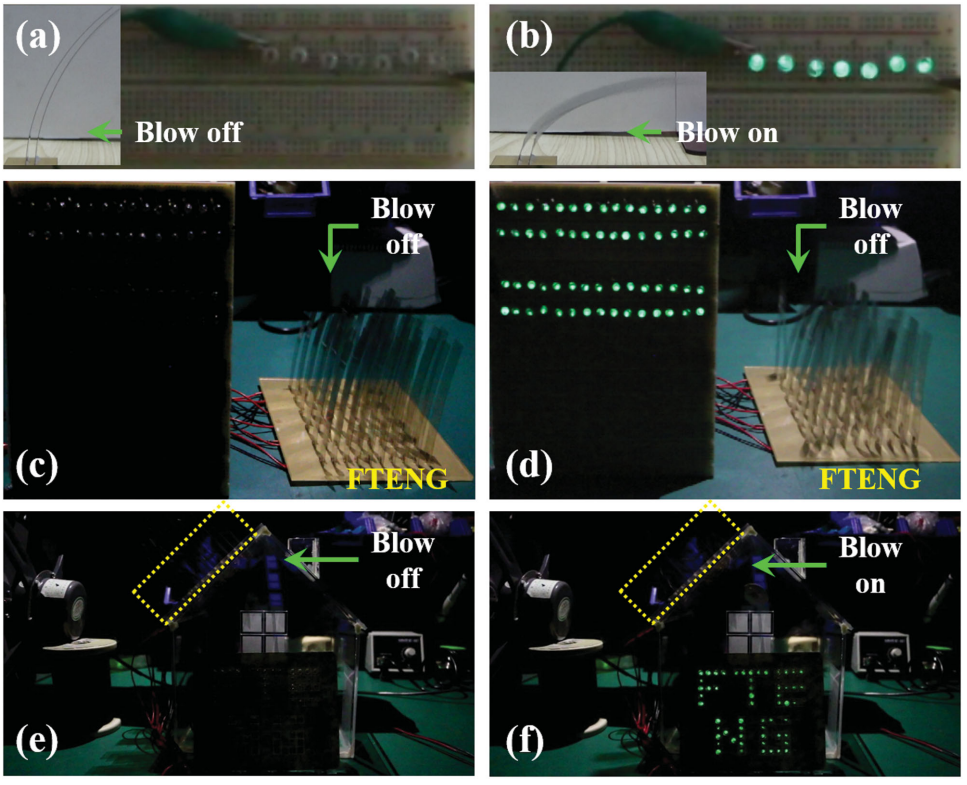

Figure 6. Demonstration of the TENG as a sustainable power source. a) Photograph that shows TENG included just two pieces of strips was working on a blower shaker. b) 7 LEDs light up simultaneously. c) Photograph of an amplificatory setup in which the TENG acted as a direct power source. d) 60 LEDs light up simultaneously. e) The self-powered house based TENG harvest wind energy all the time and f) power a display board.

© 2015 WILEY-VCH Verlag GmbH & Co. KGaA, Weinheim
Adv. Mater. **2015**,
DOI: 10.1002/adma.201504462

Acknowledgements

L.Z., B.Z., and J.C. contributed equally to this work. This work was supported by the National Natural Science Foundation of China (No. 51202023), the scientific and technological projects for Distinguished Young Scholars of Sichuan Province (No. 2015JQ0013), the Fundamental Research Funds for the Central Universities of China (A0920502051408-10), the Hightower Chair foundation, and the "thousands talents" program for pioneer researcher and his innovation team, China. The high speed camera was provided by Assoc. Prof. Jifeng Han from Sichuan University. Patents have been filed based on the research results presented in this manuscript.

Received: September 11, 2015
Revised: November 8, 2015
Published online:

[1] J. P. Painuly, *Renewable Energy* **2001**, *24*, 73.
[2] T. Ackermann, L. Söder, *Renewable Sustainable Energy Rev.* **2000**, *4*, 315.
[3] D. Weisser, R. S. Garcia, *Renewable Energy* **2005**, *30*, 1299.
[4] Z. L. Wang, J. Chen, L. Lin, *Energy Environ. Sci.* **2015**, *8*, 2250.
[5] Z. L. Wang, *ACS Nano* **2013**, *7*, 9533.
[6] S. Soh, S. W. Kwok, H. Liu, G. M. Whitesides, *J. Am. Chem. Soc.* **2012**, *134*, 20151.
[7] G. Zhu, B. Peng, J. Chen, Q. Jing, Z. L. Wang, *Nano Energy* **2015**, *14*, 126.
[8] G. Zhu, Y. Su, P. Bai, J. Chen, Q. Jing, W. Yang, Z. L. Wang, *ACS Nano* **2014**, *8*, 6031.
[9] J. Chen, J. Yang, Z. Li, X. Fan, Y. Zi, Q. Jing, H. Y. Guo, Z. Wen, K. C. Pradel, S. M. Niu, Z. L. Wang, *ACS Nano* **2015**, *9*, 3324.
[10] S. W. Thomas, S. J. Vella, M. D. Dickey, G. K. Kaufman, G. M. Whitesides, *J. Am. Chem. Soc.* **2009**, *131*, 8746.
[11] F. Yi, L. Lin, S. Niu, P. K. Yang, Z. Wang, J. Chen, Y. S. Zhou, Y. L. Zi, J. Wang, Q. L. Liao, Y. Zhang, Z. L. Wang, *Adv. Funct. Mater.* **2015**, *25*, 3688.
[12] Y. Su, X. Wen, G. Zhu, J. Yang, J. Chen, P. Bai, Z. M. Wu, Y. D. Jiang, Z. L. Wang, *Nano Energy* **2014**, *9*, 186.
[13] Y. Zi, L. Lin, J. Wang, S. Wang, J. Chen, X. Fan, P. Yang, F. Yi, Z. L. Wang, *Adv. Mater.* **2015**, *27*, 2340.
[14] G. Zhu, P. Bai, J. Chen, Z. L. Wang, *Nano Energy* **2013**, *2*, 688.
[15] X. Fan, J. Chen, J. Yang, P. Bai, Z. Li, Z. L. Wang, *ACS Nano* **2015**, *9*, 4236.
[16] J. Yang, J. Chen, Y. Liu, W. Yang, Y. Su, Z. L. Wang, *ACS Nano* **2014**, *8*, 2649.
[17] H. T. Baytekin, A. Z. Patashinski, M. Branicki, B. Baytekin, S. Soh, B. A. Grzybowski, *Science* **2011**, *333*, 308.
[18] J. Chen, G. Zhu, W. Yang, Q. Jing, P. Bai, Y. Yang, T. Hou, Z. L. Wang, *Adv. Mater.* **2013**, *25*, 6094.
[19] H. Guo, J. Chen, M. H. Yeh, X. Fan, Z. Wen, Z. Li, C. Hu, Z. L. Wang, *ACS Nano* **2015**, *9*, 5577.
[20] B. Baytekin, H. Baytekin, B. Grzybowski, *J. Am. Chem. Soc.* **2012**, *134*, 7223.
[21] W. Yang, J. Chen, G. Zhu, X. Wen, P. Bai, Y. Su, Y. Lin, Z. L. Wang, *Nano Res.* **2013**, *6*, 880.
[22] Y. Yang, H. Zhang, Z. Lin, Y. Liu, J. Chen, Z. Lin, Y. Zhou, C. Wong, Z. L. Wang, *Energy Environ. Sci.* **2013**, *6*, 2429.
[23] Y. Su, G. Zhu, W. Yang, J. Yang, J. Chen, Q. Jing, Z. Wu, Y. Jiang, Z. L. Wang, *ACS Nano* **2014**, *8*, 3843.
[24] J. Chen, G. Zhu, J. Yang, Q. Jing, P. Bai, W. Yang, X. Qi, S. Yuan, Z. L. Wang, *ACS Nano* **2015**, *9*, 105.
[25] G. Zhu, W. Q. Yang, T. Zhang, Q. Jing, J. Chen, Y. Zhou, P. Bai, Z. L. Wang, *Nano Lett.* **2014**, *14*, 3208.
[26] W. Yang, J. Chen, X. N. Wen, Q. S. Jing, J. Yang, Y. J. Su, G. Zhu, W. Z. Wu, Z. L. Wang, *ACS. Appl. Mater. Interfaces* **2014**, *6*, 7479.
[27] Y. Yang, G. Zhu, H. L. Zhang, J. Chen, X. D. Zhong, Z. H. Lin, Y. J. Su, P. Bai, X. N. Wen, Z. L. Wang, *ACS Nano* **2013**, *7*, 9461.
[28] J. Bae, J. Lee, S. Kim, J. Ha, B.-S. Lee, Y. Park, C. Choong, J. B. Kim, Z. L. Wang, *Nat. Commun.* **2014**, *5*, 4929.
[29] X. Wang, S. H. Wang, Y. Yang, Z. L. Wang, *ACS Nano* **2015**, *9*, 4553.
[30] S. Lee, S. H. Bae, L. Lin, Y. Yang, C. Park, S. W. Kim, S. N. Cha, H. Kim, Y. J. Park, Z. L. Wang, *Adv. Funct. Mater.* **2013**, *23*, 2445.
[31] O. Doare, S. Michelin, *J. Fluid Struct.* **2011**, *27*, 1357
[32] J. Yang, J. Chen, Y. J. Su, Q. S. Jing, Z. L. Li, F. Yi, X. N. Wen, Z. N. Wang, Z. L. Wang, *Adv. Mater.* **2015**, *27*, 1316.
[33] Z. Wen, J. Chen, M.-H. Yeh, H. Guo, Z. Li, X. Fan, T. Zhang, L. Zhu, Z. L. Wang, *Nano Energy* **2015**, *16*, 38.
[34] G. Zhu, J. Chen, Y. Liu, P. Bai, Y. S. Zhou, Q. S. Jing, C. F. Pan, Z. L. Wang, *Nano Lett.* **2013**, *13*, 2282.
[35] J. Yang, J. Chen, Y. Yang, H. L. Zhang, W. Q. Yang, P. Bai, Y. J. Su, Z. L. Wang, *Adv. Energy Mater.* **2014**, *4*, 1301322.
[36] H. Zhang, Y. Yang, Y. J. Su, J. Chen, C. G. Hu, Z. K. Wu, Y. Liu, C. P. Wong, Y. Bando, Z. L. Wang, *Nano Energy* **2013**, *2*, 693.
[37] X. N. Wen, W. Q. Yang, Q. S. Jing, Z. L. Wang, *ACS Nano* **2014**, *8*, 7405.
[38] Z. Li, J. Chen, J. Yang, Y. J. Su, X. Fan, Y. Wu, C. W. Yu, Z. L. Wang, *Energy Environ. Sci.* **2015**, *8*, 887.
[39] Y. Su, J. Chen, Z. M. Wu, Y. D. Jiang, *Appl. Phys. Lett.* **2015**, *106*, 013114.
[40] L. Zhang, L. Jin, B. Zhang, W. Deng, H. Pan, J. Tang, M. Zhu, W. Yang, *Nano Energy* **2015**, *16*, 516.
[41] W. Yang, J. Chen, Q. S. Jing, J. Yang, X. N. Wen, Y. J. Su, G. Zhu, P. Bai, Z. L. Wang, *Adv. Funct. Mater.* **2014**, *24*, 4090.
[42] G. Zhu, J. Chen, T. J. Zhang, Q. S. Jing, Z. L. Wang, *Nat. Commun.* **2014**, *5*, 3426.
[43] W. Yang, J. Chen, G. Zhu, J. Yang, P. Bai, Y. J. Su, Q. S. Jing, X. Cao, Z. L. Wang, *ACS Nano* **2013**, *7*, 11317.
[44] L. Feng, S. H. Li, H. J. Li, J. Zhai, Y. L. Song, L. Jiang, D. B. Zhu, *Angew. Chem. Int. Ed.* **2002**, *41*, 1221.

© 2015 WILEY-VCH Verlag GmbH & Co. KGaA, Weinheim